J. P. Soaphys, Vol 3, N°1 (2021) C21A05
http://dx.doi.org/10.46411/jpsoaphys.2021.01.05

Journal de physique de la SOAPHYS
http://www.soaphys.org/journal/
ISSN Print : *2630-0958*

MORPHOLOGICAL AND OPTICAL STUDIES OF PZN-4.5PT NANOPARTICLES THIN FILMS ON NANOSTRUCTURED SILICON SUBSTRATE

Fall Ndeye C. Y.[1, *], Touré M.[1], Ndioukane R.[1], Kobor D.[1], Pasquinelli M.[2] and, Dobbins T. A.[3]

[1]*Université Assane Seck de Ziguinchor, Laboratoire de Chimie et de Physique des Matériaux, Ziguinchor, Sénégal, n.fall1530@zig.univ.sn ; m.toure5053@zig.univ.sn; , R.NDIOUKANE1532@zig.univ.sn ; dkobor@univ-zig.sn;*

[2]*Aix Marseille Université, Institut Matériaux Microélectronique Nanosciences de Provence, Marseille, France, marcel.pasquinelli@univ-amu.fr*

[3] *Rowan University, Department of Physics & Astronomy, Chicago, USA, Dobbins@rowan.edu*

INFOS SUR L'A R T I C L E

Historique de l'article:
Reçu le : 26 novemvre 2020
Réçu en format revisé le : 30/05/2021
Accepté le : 02/10/2021

Keywords : PZN-4.5PT, spin coating, relaxor, UV-visible

ABSTRACT

The development of renewable energies is today essential to be able to respond in a sustainably way to the growing energy needs on a global scale, as well as to reduce the greenhouse gas emissions responsible for global warming. Among these energies, photovoltaic technology, which converts light power of the sun (renewable source) into electric power, is a major player in the energy transition. However, there is now a need to develop efficient, competitive and less polluting photovoltaic technologies, allowing more energy to be produced at a lower cost. The Pb ($Zn_{1/3}$ $Nb_{2/3}$) O_3 (PZN) relaxor and its solid solutions with ferroelectric $PbTiO_3$ (PT) are of considerable interest both from the applications point of view and from the scientific point of view. In the past, numerous attempts have been made to prepare and study the properties of these materials in the form of thin layers for photovoltaic applications. However, due to the difficulties in preparing pure phase films with a high PZN content, there is very little knowledge of the properties of these materials. The objective of this work is to prepare PZN-4.5PT nanoparticle thin films, to study in detail their morphological and optical properties. The studies were carried out in three main directions: preparation of thin layers (PZN-PT) by deposit of spin coating, and characterize for optical and morphological properties (SEM). UV-visible measurements allowed us to have reflectance of less than 30% after deposit a thin layer PZN-4.5PT doped 1% Mn and undoped for a 70 at 80% absorption in UV-Visible-NIR.

I. INTRODUCTION

Reducing reflectance is critical to improving the performance of the solar cells. Compared with the planar solar cells, the silicon nanowires (SiNWs) solar cells can greatly reduce reflectance. Nowadays, SiNWs arrays have been applied to nanosensors [1-2], field emission display devices [1], optoelectronic devices [3], solar cells [4-5], and lithium batteries [6-7], due to these advantages such as high surface activities, electronic transport characteristics, field emission properties and optical properties [8-9]. The reasons why SiNWs arrays have such a low reflectivity are as follows: i) high surface area of SiNWs arrays which can repeatedly scatter and absorb the incident light, ii) subwavelength light trapping effect, and iii) SiNWs arrays that are equivalent to a uniform dielectric layer whose refractive index is between that of the air and that of the silicon lead to a gradient of the refractive index from the air to the silicon. At present, there are numerous methods to synthesize SiNWs arrays including laser ablation [10-11], thermal evaporation [12-13], chemical vapor deposition (CVD) [14-15], template method, and metal-assisted chemical etching (MACE) [16-17]. The MACE method has attracted much attention because it has various advantages such as simple operation, low requirements for equipment, and easy production for large-area uniform SiNWs arrays. In 1957, Treuting and Arnold [18] first reported the whisker structure of silicon, and pointed out that the growth direction may be <111> direction. In 2006, Peng [19] fabricated well-aligned large-area SiNWs arrays using MACE method and researched the etching behavior of silicon in aqueous fluoride solution. Moreover, Zhang [20] also reported large-area uniform SiNWs arrays using the method of MACE.

In recent years, the MACE method has been widely applied to prepare SiNWs arrays. $AgNO_3$ solution, HF solution and H_2O_2 solution are used in this method. $AgNO_3$

solution is used to generate Ag nanoparticles (AgNPs), and also plays a crucial role in the formation of SiNWs arrays. HF solution can provide fluoride ions to dissolve the oxide layer so that the silicon surface can continue to be etched down. Moreover, H_2O_2 concentration directly affects the density of SiNWs arrays [19]. Therefore, the distance between SiNWs arrays can be adjusted by changing the concentration of H_2O_2. In the etching process, H_2O_2 near the surface of the AgNPs will be preferentially reduced because Ag possesses catalytic activity for the reduction of the oxidant, and the holes which are produced by the reduction reaction diffuse and inject into the silicon through AgNPs. The silicon is oxidized by the injected holes. And then the oxide layer is dissolved in the HF solution in the interface of AgNPs and silicon. However, the inorganic perovkite PZN-PT is used as an absorber of the light spectrum in the form of thin layers by a simple, easy and inexpensive method, the spin coating method at the LCPM laboratory of the Assane Seck University of Ziguinchor.

II. EXPERIMENTAL METHOD

Preparation of nanostructured silicon substrates p-Si(100), the silicon surface was first degreased in acetone and isopropanol, rinsed with water distilled, and then cleaned in a piranha solution (H_2SO_4/H_2O_2) for 10 min, followed by copious rinsing with water distilled. The nanostructured silicon surfaces were obtained by chemical etching of the clean substrate in $HF/HNO_3/AgNO_3$ aqueous solution at room temperature. For $AgNO_3$ concentration of 0.02 M, the etching time is 30 min. The resulting surfaces were rinsed copiously with deionized water and immersed in an aqueous solution of $HCl/HNO_3/H_2O$ (1/1/1) overnight at room temperature to remove the silver nanoparticles and dendrites deposited on the surface during the chemical etching. Then introduce the samples in a new $AgNO_3$ solution for 15 min to be able to reproduce a new form of morphology obtained in other studies in our LCPM laboratory.

The grounded powder was dispersed in a gel fabricated in the laboratory LCPM in Assane Seck University of Ziguinchor. To obtain a homogeneous film, spin coating process was carried out at room temperature using a spin coater Midas 1200D model at 3500 rpm with an initial acceleration of 5 seconds and an operating time of 10 min. After 10 min bake in oven at 100˚C (at 100˚C there is good adhesion of the deposited thin layer as shown by D. Kobor et al .), thermal annealing in a K114 type muffle furnace was performed. Heating was carried out at 900˚C for the gel diffusion through the p-type silicon nanowires with a heating rate between 10 and 20˚C/min and 30 - 60 min plateau. Different samples were fabricated using the two types of nanopowders (undoped PZN-4.5PT powder and 1% Mn PZN-4.5PT doped powder) and characterized. Surface morphology and composition of Si samples were observed respectively by using a MERLIN FEG of Zeiss scanning electron microscopy and energy dispersive X-ray spectrometry (EDX) model in ICMPE (Aix Marseille). The total reflectance for normal incidence was measured using a spectrophotometer with an integrating sphere model in LAMBDA 950S integrat in sphere in IM2NP (Aix-Marseille).

III. RESULTS AND DISCUSSION

3.1 SEM images

Figures 1 and 2 shows the SEM images respectively a textured surface and thin layers of PZN-4.5PT nanoparticle (doped and undoped). The results are on the SEM images of fig. 1. This etching made it possible to obtain sparingly dense inverted pyramids (with the Ag catalyst) with sizes varying from 100 to 700 nm approximately (for the HF / $AgNO_3$ ratio of 4, 8 / 0.02 for 30 minutes).

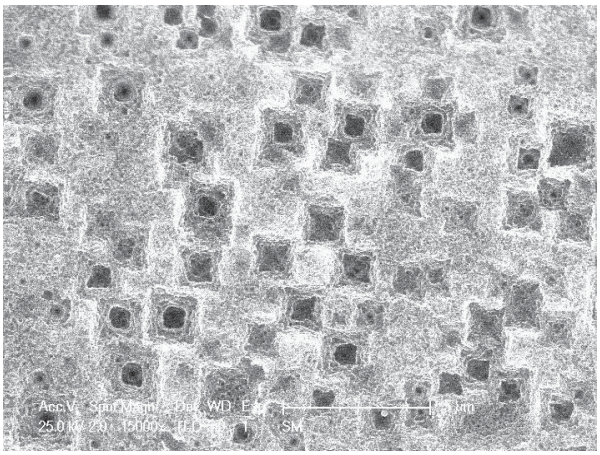

Figure 1. SEM images of p type Silicon inverted nanopyramides.

Fig. 2 presents the SEM images of the deposition of the thin gel layer and of nanoparticles of PZN-4.5PT (fig 2.a) and PZN-4.5PT + 1% Mn (fig. 2.b) on the inverted nanopyramides. We observe an irregularity of the layer, shown by the presence of light areas and dark areas. It is necessary to note the formation of dark circles inside which there is overgrowth on the thin layer of a new phase consisting of crystals of hexagonal shape shown in yellow arrow. The lightest areas correspond to the areas where the gel containing the perovskite is most dense and where it has crystallized. These nanostructures mix with perovskite (doped and undoped) to form microcrystals.

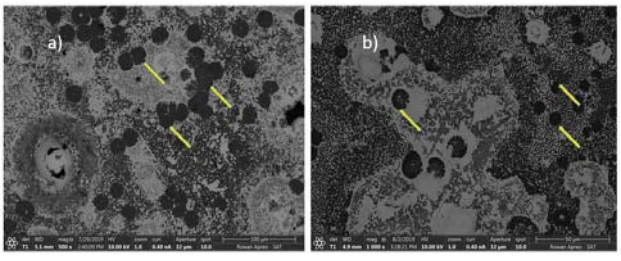

Figure 2. SEM images of thin layers of PZN-4.5PT nanoparticle a) undoped and b) doped 1% Mn of inverted nanopyramides.

3.2 Optical properties

To more precisely assess the optical properties of the layer of Perovskite nanoparticles (undoped and Mn-doped PZN-4.5PT), measurements by UV-Visible spectroscopy were carried out. The reflection and absorption spectra of the PZN-4.5PT thin films (Fig. 3) and PZN-4.5PT undoped (Fig.4) deposited on a nanotextured silicon substrate show a high reflection (more than 20%) see fig. 3 (a) and fig. 4 (a) in the visible range (~ 400 - 1200 nm). This reflectance high behavior they thin films from perovskite nanoparticles could be explained by the high reflectance values of PZN-PT single crystals (20% - 25%) [21]. An absorption of approximately over 70 to 80% observed for all doped and non-doped films (Figure 3 (b) and Figure 4 (b)) in the UV, Visible and near infrared regions. Absorption widens almost across the wavelength range (UV-Visible-NIR). These results allow achieving good absorption materials over the entire useful wavelength, for photovoltaic conversion efficiency improvement.

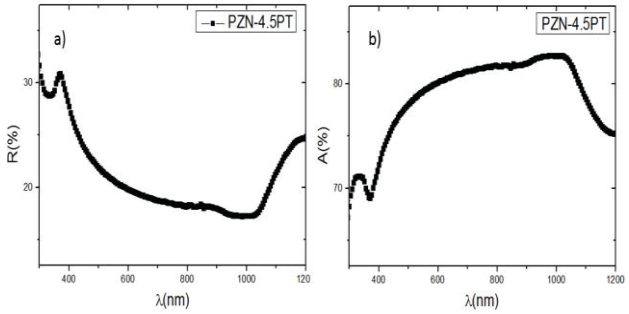

Figure 3. (a) Reflectance and (b) absorbance for thin layers of undoped PZN-4.5PT nanoparticles

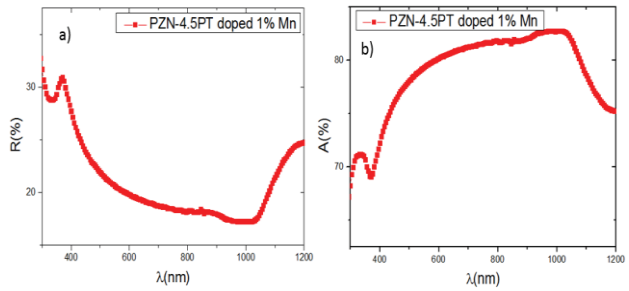

Figure 4. (a) Reflectance and (b) absorbance for thin layers of doped 1% Mn PZN-4.5PT nanoparticles

3.3 Chemical composition analysis (EDX, Mapping)

Figure 5 (a-g) shows the SEM-EDX analysis of the chemical composition of PZN-4.5PT nanoparticles doped 1% Mn on nanostructured silicon substrate. In figure 5 (h) we have the representation of the signal intensity of the different chemical elements present on the surface as a function of the depth. An EDX analysis coupled with SEM enabled the presence of the different chemical elements of the PZN-4.5PT nanoparticle to be demonstrated. The SEM-EDX images of Figures 5 (a) - (b) correspond respectively to the distribution of silicon and oxygen, which respectively reflects the presence of nanostructures silicon with the silicon substrate (SiO_2) and oxygen with the presence of the gel or SiO_2. Images (c) - (e) - (f) - (g) for their part correspond to the distribution of lead, Plomb, Zinc of Niobate and Titanium, representative of the thin film of PZN-4.5PT deposited by spin coating on a textured silicon substrate. Image (d) represent the distribution of phosphorus which also reflects the presence of the phosphorus gel mixed at the base with the perovskite. It can be seen that the PZN-4.5PT nanoparticle is deposited all along the silicon nanostructures. All the elements, representative of perovskite, are present throughout the mapping, indicating the infiltration of the solution along the textured silicon substrates. The proof, in figures 5.(h) showing the signal intensity strokes/ second as a function of the depth of the thin film PZN-4.5PT + 1% Mn and PZN-4.5PT respectively. Different chemical elements depending on the depth (0-22µm) are present throughout the depth of the sample. The infiltration seems homogeneous throughout its thickness.

By comparison with the EDX measurements carried out on the same sample thin film doped to know the different elements which constitute the layer of nanoparticles of PZN-4.5PT. Several sites (12, 13, 14, and 15) on the sample were chosen (Figure 5a).

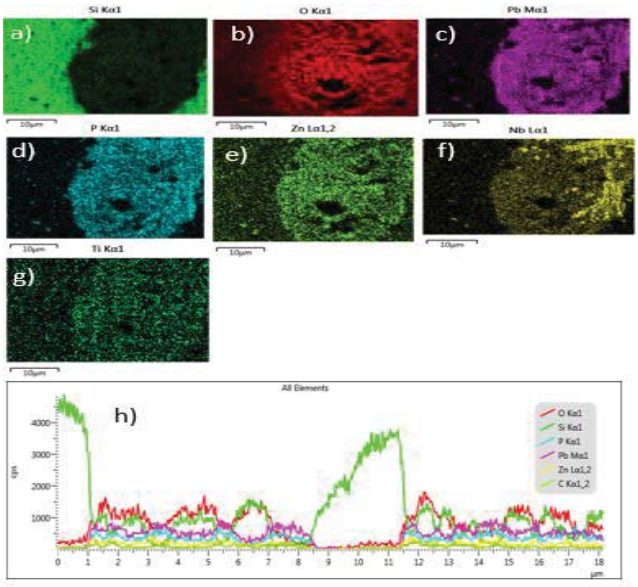

Figure 5. (a), (b), (c), (d), (e), (f) and (g) SEM-EDX of PZN-4.5PT +1% Mn nanoparticle on an inverted nanopyramid surface (h) Distribution profile of chemical elements.

The EDX results (Figure 6.b, c, d et e) of the sample show that this layer is mainly composed of the various elements that constitute the layer of nanoparticles of [Pb ($Zn_{1/3}$ $Nb_{2/3}$) O_3-4.5 % $PbTiO_3$ (PZN-4.5%PT)] doped 1% Mn on the surface of nanostructured silicon, with traces of oxygen, fluorine, carbon.

The use of deionized water and / or acids (HNO_3, HCl, H_2SO_4) at the end of the chemical attack process for nanostructured silicon could explain the presence of chemical impurities such as (Ca^{2+}, F^-, Na^+, K^+, Al^{3+}).

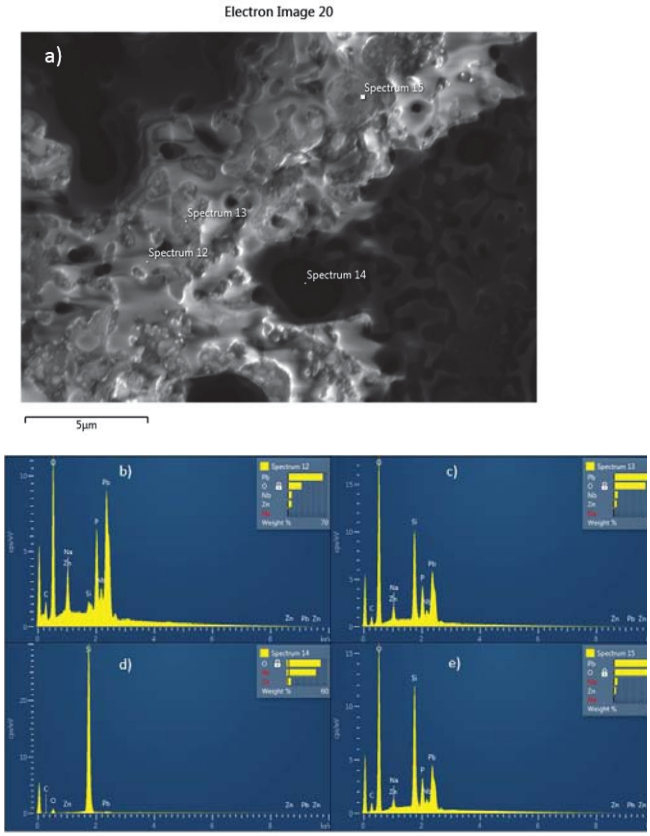

Figure 6. Distribution of atoms on the surface of a layer of nanoparticles a) PZN-4.5PT+1%Mn b) c) d) et e) EDX measurements

The 1% Mn doping has no influence on the morphological and optical properties of the thin layers of PZN-4.5PT nanoparticles. The low proportion of 1% Maganesis may explain the absence of a peak corresponding to Mn on the SEM-EDX measurements.

IV. CONCLUSION

PZN-4.5PT nanoparticles thin layers were prepared using a gel fabricated in our laboratory. Silicon p-type nanostructured was used to deposit this thin film. SEM images revealed fairly homogeneous distribution of the gel inside the inverted nanopyramids. Optical properties investigation shows very good absorption for all the thin films in UV, Visible and NIR. Which shows that these reflection results confirm the possible use of such materials as antireflective thin layers.

ACKNOWLEDGEMENTS

This work is supported by the French Embassy for the French cooperation grant, the Im2np team from Marseille and ANL from Chicago.

REFERENCES

[1] E. Stern, R. Wagner, R. Breaker, Nano Letters, 7 (2007) 3405-3409.

[2] M. Jeon, K. Kamisako, Mater Lett. 63(9-10) (2009) 777-779.

[3] Y. Qu, L. Liao, Y. Li, H. Zhang, Y. Huang, X. Duan, Nano Lett. 9(12) (2009) 4539.

[4] X.Q. Bao, C.M. Fatima, P. Alpuim, L. Liu, Chem Commun. 51(53) (2015) 10742-5.

[5] P. Yang, Semiconductor nanowires for energy conversion, Nanoelectronics Conference, 2010, pp. 49-49.

[6] M. Ge, J. Rong, X. Fang, A. Zhang, Y. Lu, C. Zhou, Nano Res. 6(3) (2013) 174-181.

[7] Y. Lu, A. Lal, Nano Lett. 10(11) (2010) 4651-4656.

[8] A.I. Hochbaum, D. Gargas, Y.J. Hwang, P. Yang, Nano Lett 9. (10) (2011) 3550-3554.

[9] Y. Wu, J.J. Hu, Y. Xu, K.Q. Peng, J. Zhu, Acta Energiae Solaris Sinica. 27(8) (2006) 811-818.

[10] Y. Cui, X.F. Duan, J.T. Hu, C.M. Lieber, J Phys Chem B. 104(22) (2000) 5213-5216.

[11] Y.F. Zhang, Y.H. Tang, N. Wang, D.P. Yu, C.S. Lee, I. Bello, S.T. Lee, Appl Phys Lett. 72(15) (1998) 1835-1837.

[12] H. Pan, S. Lim, C. Poh, H. Sun, X. Wu, Y. Feng, J. Lin, Nanotechnol. 16(16) (2005) 417.

[13] Z. W. Pan, Z. R. Dai, L. Xu, S. T. Lee, and, Z. L. Wang, §, J Phys Chem B. 105(13) (2001) 2507-2514.

[14] M. Lu, M.K. Li, L.B. Kong, X.Y. Guo, H.L. Li, Chem Phys Lett. 374(5–6) (2003) 542-547.

[15] T. Stelzner, M. Pietsch, G. Andrä, F. Falk, E. Ose, S. Christiansen, Nanotechnol. 19(29) (2008) 295203.

[16] Z. Huang, H. Fang, J. Zhu, Adv Mater. 19(5) (2007) 744-748.

[17] K. Peng, M. Zhang, A. Lu, N.B. Wong, R. Zhang, S.T. Lee, Appl Phys Lett. 90(16) (2007) 163123-163123-3.

[18] R.G. Treuting, S.M. Arnold, Acta Metallurgica 5(10) (1957) 598-598.

[19] K.P. Dr, H. Fang, J. Hu, Y. Wu, Z.P. Jing, Y. Yan, S.T.L. Prof, Chemistry (Weinheim an der Bergstrasse, Germany) 12(30) (2006) 7942-7.

[20] Mingliang Zhang, Kuiqing Peng, X. Fan, Jiansheng Jie, Ruiqin Zhang, A. Shuittong Lee, Ningbew Wong, J Phys Chem C. 112(12) (2008) 4444-4450.

[21] Kobor, D., Tine, M., Hajjaji, A., Lebrun, L. and Guyomar, D. Journal of Modern Physics, 2012, 3, 402-409.